DEUTSCHES ELEKTRONEN-SYNCHROTRON DESY

DESY 80/01
January 1980

TEST OF QED IN THE REACTIONS $e^+e^- \to e^+e^-$ AND $e^+e^- \to \mu^+\mu^-$ AT CMS ENERGIES FROM 9.4 TO 31.6 GeV

by

PLUTO Collaboration

NOTKESTRASSE 85 · 2 HAMBURG 52

To be sure that your preprints are promptly included in the
HIGH ENERGY PHYSICS INDEX ,
send them to the following address (if possible by air mail) :

DESY
Bibliothek
Notkestrasse 85
2 Hamburg 52
Germany

DESY 80/01
January 1980

TEST OF QED IN THE REACTIONS $e^+e^- \to e^+e^-$ and $e^+e^- \to \mu^+\mu^-$ AT CMS ENERGIES FROM 9.4 TO 31.6 GEV

PLUTO Collaboration

Ch. Berger, H. Genzel, R. Grigull, W. Lackas and F. Raupach
I. Physikalisches Institut der RWTH Aachen[1], Germany

A. Klovning, E. Lillestöl, E. Lillethun and J.A. Skard
University of Bergen[2], Norway

H. Ackermann, G. Alexander[3], F. Barreiro, J. Bürger, L. Criegee, H.C. Dehne, R. Devenish[4], A. Eskreys[5], G. Flügge[9], G. Franke, W. Gabriel, Ch. Gerke, G. Knies, E. Lehmann, H.D. Mertiens, U. Michelsen, K.H. Pape, H.D. Reich, B. Stella[6], T.N. Ranga Swamy[7], U. Timm, W. Wagner, P. Waloschek, G.G. Winter and W. Zimmermann
Deutsches Elektronen-Synchrotron DESY, Hamburg, Germany

O. Achterberg, V. Blobel[8], L. Boesten, H. Kapitza, B. Koppitz, B. Lewendel, W. Lührsen, R. Maschuw[9], R. van Staa and H. Spitzer
II. Institut für Experimentalphysik der Universität Hamburg[1], Germany

C.Y. Chang, R.G. Glasser, R.G. Kellogg, K.H. Lau, B. Sechi-Zorn, A. Skuja, G. Welch and G.T. Zorn
University of Maryland[10], College Park, USA

A. Bäcker, S. Brandt, K. Derikum, A. Diekmann, C. Grupen, H.J. Meyer, B. Neumann, M. Rost and G. Zech
Gesamthochschule Siegen[1], Germany

T. Azemoon[11], H.J. Daum, H. Meyer, O. Meyer, M. Rössler, D. Schmidt and K. Wacker[12]
Gesamthochschule Wuppertal[1], Germany

(Submitted to Zeitschrift für Physik C)

1) Supported by the BMFT, Germany
2) Partially supported by the Norwegian Research Council for Science and Humanities
3) On leave from Tel Aviv University, Israel
4) Now at Oxford University, England
5) On leave from Institute of Nuclear Physics, Krakow, Poland
6) On leave from University of Rome, Italy; partially supported by INFN
7) On leave from Tata Institute, Bombay, India
8) Now at CERN, Geneva, Switzerland
9) Now at Institut für Experimentelle Kernphysik, Karlsruhe, Germany
10) Partially supported by Department of Energy, USA
11) Now at University College, London, England
12) Now at Harvard University, Cambridge, Mass., USA

Abstract

We have measured Bhabha scattering at cms energies of 9.4, 13, 17, 22, 27.5, 30.0 and 31.6 GeV and the reaction $e^+e^- \rightarrow \mu^+\mu^-$ at 9.4 GeV. The experiment covers spacelike momentum transfers up to - 850 GeV^2 and timelike momentum transfers up to 1000 GeV^2. We obtain good agreement with QED comparing differential cross sections (measured between 35^0 and 145^0), acoplanarity distributions and the energy dependence (for Bhabha scattering). Defining possible modifications of QED in a model independent way we obtain stringent limits in the range of 70 - 200 GeV on cutoff parameters. We test to an accuracy of 5 - 8 % the validity of some general principles of QED, such as pointlike coupling, crossing symmetry and μe- universality.

1. Introduction

Electron - positron storage rings allow for testing the validity of QED in purely electromagnetic processes at large momentum transfers. With the high energies reached at PETRA these tests can be extended into a largely increased kinematical region. Using the detector PLUTO we have measured Bhabha scattering at time- and spacelike momentum transfers up to 1000 and -850 GeV^2, respectively. This allows us to probe the pointlike structure of the electron down to distances of $\sim 10^{-16}$cm. The sensitivity of the experiment to modifications of the timelike amplitude rests largely on the available charge identification, which enables measurements at backward scattering angles up to 145^0, where QED violations are most likely to show up. Since our data cover overlapping q^2 ranges at different energies it is possible to apply a model independent parametrization of possible QED modifications according to the most recent discussions of the subject (18).

We include in the present QED test our data on $e^+e^- \rightarrow \mu^+\mu^-$ at E_{cms} = 9.4 GeV. The combined muon and electron data are used in order to test μe-universality and to constrain the timelike form factor. The crossing symmetry of the scattering and annihilation amplitudes is also tested. Previous QED checks using the reactions $e^+e^- \rightarrow e^+e^-$ and $e^+e^- \rightarrow \mu^+\mu^-$ have been performed at ADONE (1), CEA (2), DORIS (3), SPEAR (4, 5) and PETRA (6).

2. Data Taking and Event Analysis

The data reported here have been taken at the e^+e^- storage rings DORIS and PETRA in Hamburg at center of mass energies of 9.4 GeV (DORIS data), 13, 17, 22, 27.5, 30.0 and 31.6 GeV (PETRA data) using the same apparatus. Bhabha scatters have been detected in the inner track detector of PLUTO (7) and in the surrounding shower counters. The inner track detector consists of a set of cylindrical proportional chambers operating in a magnetic field of 1.65 T. They provide a momentum resolution for hadrons of $\sigma_p/p = 3\,\% \cdot p$ above 3 GeV. The momentum resolution of electrons is poorer by a factor of two due to radiative energy losses. The chambers are surrounded by a double layer of lead scintillator shower counters (barrel) of 8.6 radiation lengths (8). The ends of the cylinder are covered by a second set of shower counters (endcaps) of 10.6 radiation lengths (9). The shower counters provide an electron energy resolution of $\sigma_E/E = 35\,\% / \sqrt{E}$ for the barrel and $\sigma_E/E = 19\,\% / \sqrt{E}$ for the endcaps (E in GeV).

A double layer of helix-tubes (10) between the two layers of the barrel counters gives an angular resolution for electromagnetic showers of $\sigma_\phi = 1.3^0$ and $\sigma_\theta = 1.4^0$, while a set of proportional chambers in the endcaps (11) allows for measuring θ with an accuracy of $\sigma_\theta = 1^0$. The endcap shower counters and proportional chambers have a segmentation in ϕ of 12^0 yielding a resolution of $\sigma_\phi \simeq 4^0$. Here θ denotes the polar angle and ϕ the azimuthal angle of the scattered e^+ relative to the e^+ beam direction.

The trigger for Bhabha scattering was a coincidence of at least twice 1.2 GeV deposited in opposite sides of the shower counter or more than 3 GeV in the counters as a whole for runs at energies below 22 GeV. The thresholds were doubled for the 27-31 GeV runs. An independent trigger demanding two coplanar tracks was used for cross checks. The resulting trigger efficiency for $e^+e^- \rightarrow e^+e^-$ events was 99.9 ± 0.1 %. The events accepted by the trigger were passed through a track recognition procedure, a vertex fit and a shower recognition program. The shower recognition program formed clusters from neighbouring shower counter signals, computed the energy deposited and combined all information available to give an optimal shower position. Candidates were accepted if they had two showers with more than one third of the beam energy each.

The events were classified as <u>one prongs</u> if only one shower had one or several tracks pointing to it, otherwise they were classified as <u>two prongs</u>. This class includes events with more than two tracks due to showering in the track detector. Events with more than four tracks from a common vertex or with no tracks pointing to the showers were rejected. For the final sample of Bhabha events an acollinearity of less than 15^0 in spatial angle was demanded using the angular information from tracks whenever available and from the shower clusters otherwise. The total efficiency for recognizing an $e^+e^- \rightarrow e^+e^-$ event was determined to be 99.3 ± 0.4 %.

A small fraction (∿ 5 %) of the detected Bhabha scatters had two tracks with the same charge assignment due to measurement errors in the track curvature. For the final cos θ distributions the events with the same charge assignment were divided according to the measured ratio of forward to backward scatters. This introduces an uncertainty of ± 6 % in the cross section for backward scatters. By comparing the number of events with opposite and same charges, we determined the probability of misidentifying the charges of <u>both</u> tracks. In the 9.4 GeV data it was found to be less than 0.1 %, even at production angles near $|\cos\theta| = 0.8$, while with increasing energy (≥ 17 GeV) we had to subtract a few events in the extreme backward region of $-0.8 < \cos\theta < -0.7$.

From the vertex distribution of the events (see Fig. 2 of ref. 7) we conclude that the background due to cosmic rays and beam gas interactions is 0.1 ± 0.05 %. The class of one prongs was scanned visually to remove background mainly due to the reaction $e^+e^- \rightarrow \gamma\gamma$, where one γ converted in the inner detector. Using the number of events with one converted γ, the contamination of the final sample by the reaction $e^+e^- \rightarrow \gamma\gamma$, where both photons converted, was calculated to be 0.3 ± 0.03 %.

These numbers were checked by inspecting visually all backward scattered $e^+e^- \rightarrow e^+e^-$ events. The inclusion of other potential background sources ($ee \rightarrow \tau\tau$, $ee \rightarrow ee\,ee$ etc.) resulted in a total contamination of 0.5 ± 0.2 % for $E_{cms} < 20$ GeV and 0.9 ± 0.3 % for $E_{cms} > 20$ GeV. We have assigned a conservative limit of 2 % to possible event losses in data handling. A summary of all corrections and systematic uncertainties is given in Table 1. Figs. 1 (a) - (f) show the angular distributions obtained after applying these corrections.

3. QED Test

3.1. Bhabha Scattering

Next we compare the data with the QED cross section for Bhabha scattering. The first order cross section has been modified by second order radiative corrections (12, 13) and the finite angular resolution of the inner detector. The radiative corrections are small varying from + 1.3 % (+ 3.5 %) at cos θ = 0.75 to - 2.3 % (-0.7 %) at cos θ = -0.3 for E_{cms} = 9.4 GeV (31.6 GeV). Here we have included the hadronic and heavy lepton vacuum polarization *, an effect which was suggested by R.P. Feynman as long as thirty years ago (14). The so modified QED angular distribution was normalized to the data in the angular range $-0.8 < \cos\theta < 0.775$. The resulting curves are shown in Fig. 1. We find good agreement with the data. The values of χ^2/DF are given in Table 2. Table 2 also contains the ratio of the integrated luminosities derived from the curves in Fig. 1 (one parameter fit) and those derived from the small angle monitor. The values agree with unity within the 9 % systematic uncertainty of the ratio.

A further check of QED has been performed by comparing the acoplanarity distribution with the QED expectation. For this purpose we have generated Bhabha events including the radiation of hard photons with a Monte Carlo program already tested at lower energies (3). Each particle was traced through the detector. The solid curve in Fig. 2 shows the expected distribution of the acoplanarity angle α from the Monte Carlo program at E_{cms} = 9.4 GeV. It agrees well with the data. In particular we find 132 events with $5^0 < \alpha < 15^0$, whereas the Monte Carlo sample yields 159 ± 11 events. A good agreement is found at the higher energies, too.

---

*) The contribution of the hadronic and heavy lepton vacuum polarization amounts to +1.9 % (+3.5 %) at cos θ = 0.75 and +3.1 % (+4.9 %) at cos θ = -0.3 for E_{cms} = 9.4 GeV (31.6 GeV). It partially cancels with the soft and hard photon radiation contributions.

To establish quantitative limits on the validity of QED one usually introduces form factors $F_T(s)$ and $F_S(q^2)$ into the amplitude for Bhabha scattering. F_T and F_S describe possible QED modifications in the eγ vertex function and/or the photon propagator for timelike and spacelike photons, respectively (15 - 17). The modified QED cross section for Bhabha scattering then reads

$$(1) \qquad \frac{d\sigma}{d\Omega} = \frac{\alpha^2}{2s}\left\{\frac{q'^4 + s^2}{q^4}|F_S|^2 + \frac{2q'^4}{q^2 s}\,\mathrm{Re}\,(F_S F_T^*) + \frac{q'^4 + q^4}{s^2}|F_T|^2\right\}(1 + \delta_{rad}(s, \theta))$$

where $s = 4\,E_{beam}^2$, $q^2 = -s\,\sin^2\frac{\theta}{2}$, $q'^2 = -s\,\cos^2\frac{\theta}{2}$ and δ_{rad} is the radiative correction.

We have the following reasons to assume that any effect of a potential QED modification must be small and $F_S, F_T \approx 1$. Since the Bhabha cross section is dominated by spacelike photon contributions, the agreement of the QED curve with the data of Fig. 1 and the overlapping of the q^2 ranges covered at the different energies support that $F_S \approx 1$. Furthermore our data on $e^+e^- \to \mu^+\mu^-$ at 9.4 GeV (see below) and that of ref. 6 agree with the QED cross section which has timelike contributions only. This supports $F_T \approx 1$.

Since both F_T and $F_S \approx 1$ we can expand F_T and F_S in a general way (18) as

$$(2) \qquad F_T(s) \simeq 1 \pm \frac{s}{\Lambda_{T\pm}^2} \quad \text{and} \quad F_S(q^2) \simeq 1 \pm \frac{q^2}{\Lambda_{S\pm}^2} .$$

The Λ's are usually referred to as cutoff parameters+). The plus and minus signs can be interpreted in terms of different ways of formulating a modified QED (17).

+) Our parametrization is the same as in ref. 4a. Note that the parametrization of ref. 5 $F(Q^2) = 1 \pm Q^2/(Q^2 - \Lambda_\pm^2) \sim 1 \mp Q^2/\Lambda_\pm^2$ with $Q^2 = q^2$ or s leads to an opposite sign convention. I.e. Λ_+ from ref. 5 should be compared to Λ_- in our paper. Ref. 6 has the same sign convention as our paper.

As mentioned above, the cross section is dominated by spacelike photons ($q^2 = -s\,\sin^2\frac{\theta}{2}$), but the relative contribution of the timelike diagram (including interference) rises, for instance, from 6.4 % at 30^0 to ~ 43 % at 150^0 scattering angle. Since we measure the angular distribution of e^+e^- scattering in a sufficiently wide angular region (from 35^0 to 145^0) and for different values of s, this makes us sensitive to the behaviour of the form factor in the spacelike and in the timelike region.

In order to determine the cutoff parameters we have fitted the data of Fig. 1 with the modified cross section (eq. 1) in the region $-0.8 < \cos\theta < 0.7$. In practice, we put $F_T(s) = 1 + \kappa_T s$ and $F_S(q^2) = 1 + \kappa_S q^2$, where κ_T, κ_S are real numbers to be fitted and $|\kappa_T| = \frac{1}{\Lambda_T^2}$, $|\kappa_S| = \frac{1}{\Lambda_S^2}$, i.e. we let the fit select the sign in eq. (2) required to describe the data. The finite errors of the fitted parameters allow the derivation of upper limits on both Λ_+ and Λ_- (see caption of Table 3). The normalization was a free parameter at each energy. In the fits the systematic uncertainties of the angular distribution and the angular resolution have been taken into account.

The fit values for κ at seven different energies (assuming from crossing symmetry $\kappa = \kappa_S = \kappa_T$) are shown in Fig. 3 (full points). The open points is the result of a previous experiment with charge identification (4a). The results are compatible with QED ($\kappa = 0$).

Next we performed overall fits including the complete set of data and treating the κ's as the only parameters. The normalization was fixed in the interval $0.7 < \cos\theta < 0.8$ assuming $F_T = F_S = 1$. This procedure is justified since for the interval $0.7 < \cos\theta < 0.8$ the momentum transfer q^2 is in a range where QED has already been tested (4, 5). Furthermore the good agreement of our differential cross sections at 9.4 and 13 GeV with QED over the full angular range supports the above procedure for the higher energies. Two separate fits assuming $\kappa_S = \kappa_T$ and $\kappa_S \neq \kappa_T$ were made. The resulting 95 % c.l. lower limits for $\Lambda_{S,T}$ are shown in Table 3 (lines 2 and 3). The results will be discussed in sec. 4

3.2. The reaction $e^+e^- \to \mu^+\mu^-$

We have also measured the reaction $e^+e^- \to \mu^+\mu^-$ at $E_{cms} \approx 9.4$ GeV using the experimental procedure described in detail in a previous paper (19). The data sample consists of 62 ± 8 events. The detection efficiency has been estimated to be (95 ± 5)%. For the determination of the absolute cross section we use the luminosity measured with the wide angle Bhabha scatters in the same runs. The radiative correction δ_{rad} (s) has been computed according to ref. 12 including a contribution of $\sim + 2.3$ % from hadronic and heavy lepton vacuum polarization (13). The angular distribution is shown in Fig. 4. The full curve is the radiatively corrected QED differential cross section folded with our angular resolution. The agreement is good.

We parametrize possible modifications of the photon propagator and/or the eγ and μγ vertex functions with the form factor $F_{T\mu}$ (s) for the timelike amplitude. Since the first order QED cross section agrees well with the data of Fig. 4, any possible deviation of $F_{T\mu}$ from unity must be small and we again can expand

$$F_{T\mu} \approx 1 \pm \frac{s}{(\Lambda^2_{T\pm})_\mu}$$

By fitting the $\mu^+\mu^-$ results with the modified QED cross section (for $m_\mu^2 \ll s$)

$$\frac{d\sigma}{d\Omega} = \frac{\alpha^2}{4s}\left[1 + \cos^2\theta\right](1 + \delta_{rad}(s))|F_{T\mu}(s)|^2 \qquad (3)$$

we get the lower limits (95 % c.l.) on $(\Lambda_{T\pm})_\mu$ shown in table 3 (line 1).

3.3. Combined Fit

In addition we performed a combined fit including the muon and Bhabha data with two different assumptions:

1) lepton universality ($\kappa_{Te} = \kappa_{T\mu}$),
2) crossing symmetry ($\kappa_S = \kappa_T$) and lepton universality.

In all cases the form factors are consistent with one. The resulting lower limits on Λ are given in Table 3 (lines 5 and 6). The difference between the lower limits for Λ_+ and Λ_- could be due to a statistical fluctation or a presently unknown systematic effect .

4. Analysis of the results and conclusions

The physical interpretation of the results with our parametrization of eventual modifications of QED is possible along the lines of refs. (15) - (18)(pointlike coupling, negative metric, heavy photon, etc.) or according to some detailed model. Here we want to check the QED photon propagator, the lepton-photon vertex function and the most general underlying assumptions of QED as the pointlike structure of leptons, crossing symmetry and lepton universality.

The form factors F_S, F_T can be thought as a product of a form factor V for the electron (muon) vertex and a form factor P for the photon propagator:

$$F_S = P_{S\gamma} V^2_{Se}, \quad F_{Te} = P_{T\gamma} V^2_{Te}, \quad F_{T\mu} = P_{T\gamma} V_{Te} V_{T\mu}.$$

QED, with single coupling (no "seagull" graph) and with pointlike leptons, has of course, V = P = 1. For any QED modification allowed by gauge and Lorentz invariance, one expects from analyticity and crossing symmetry that V_{Te} should behave like V_{Se} ($V_{Te}(s) = V_{Se}(q^2)$) in the physical region(20). Finally, if lepton universality is valid, $V_{T\mu} = V_{Te}$.

If leptons are extended, one would expect the following modification of the photon propagator * (16)

$$-\frac{1}{q^2} \to -\frac{1}{q^2} + \frac{1}{q^2-\Lambda^2} \approx -\frac{1}{q^2}\left(1 + \frac{q^2}{\Lambda^2}\right)$$

---

* In this case the Coulomb potential would be modified in the static limit (for r < 1/Λ = 1 and ħ = c = 1) via
$\frac{1}{r} \to \frac{1}{r}(1 - e^{-\Lambda r})$ (Λ ≡ "cutoff parameter")

In order to estimate the effect to the propagator we assume that a possible QED modification is due to the propagator alone and not due to the vertex function (i.e. $V = 1$). We further assume crossing symmetry, i.e. $P_{S\gamma} = P_{T\gamma} \equiv P$. Hence we can set $F = P = 1 + q^2/\Lambda^2$ and we obtain at the maximum (timelike) momentum transfer

$$P = 1 + \kappa_e\, s = 1.085 \, {}^{+\,0.054}_{-\,0.058} \, .$$

Our cutoff values correspond to having probed the electron structure down to distances of

$$l_e \approx \frac{1}{\Lambda_{e+}} \leq 2.5 \quad 10^{-16}\text{cm} \qquad (95\ \%\ \text{c.l.})$$

and the muon structure down to

$$l_\mu \approx \frac{1}{\Lambda_{\mu+}} \leq 9.5 \quad 10^{-16}\text{cm} \qquad (95\ \%\ \text{c.l.}).$$

On the other hand, assuming $P = 1$, we find for the lepton-photon vertex functions (in the "worst" case ≡ highest available momenta):

$$V_{Se} = \sqrt{1 + \kappa_{Se}\, q^2} = 0.95 \pm 0.03$$

$$V_{Te} = \sqrt{1 + \kappa_{Te}\, s} = 1.002 \, {}^{+\,0.072}_{-\,0.075}$$

and, assuming $V_{Te} = 1$

$$V_{T\mu} = 1 + \kappa_{T\mu} s = 1.03 \pm 0.06$$

Without any assumption, at the highest momentum transfers, we have

$$F_S = 0.91 \, {}^{+\,0.06}_{-\,0.05} \, , \quad F_{Te} = 1.00 \, {}^{+\,0.14}_{-\,0.15} \, , \quad F_{T\mu} = 1.03 \, {}^{+\,0.06}_{-\,0.05} \, .$$

In order to test analyticity and crossing symmetry, one can study the ratio $A = F_{Te} / F_{Se}$ as a function of energy, but with $|q^2| = s$ ($s \leftrightarrow t$ interchange). For estimating the effect we assume $P = 1$, $s = |q^2_{max}|$) and obtain:

$$A = \frac{V_{Te}}{V_{Se}} = \sqrt{\frac{1 + \kappa_{Te} s}{1 + \kappa_{Se} q^2}} = 1.051 \, {}^{+\,0.061}_{-\,0.064} \, .$$

The validity of crossing symmetry can be tested quantitatively also defining

$$\frac{1}{C^2} = \left| \frac{1}{\Lambda_S^2} - \frac{1}{\Lambda_T^2} \right| = (0.9 \pm 1.9)\ 10^{-4}.$$

As a lower limit for C we get 55 GeV at 95 % c.l..

In order to check μe-universality we define similarly

$$\frac{1}{U^2} = \left| \frac{1}{\Lambda_{T\mu}^2} - \frac{1}{\Lambda_{Te}^2} \right| = (0.33 \, {}^{+0.62}_{-0.72})\ 10^{-3}$$

and obtain $U > 21$ GeV (95 % c.l.) More directly, for the ratio

$$T = \frac{F_{T\mu}}{F_{Te}} = \frac{V_{T\mu}}{V_{Te}}$$

we get at $s = 88.2\ \text{GeV}^2$:

$$T = \frac{V_{T\mu}}{V_{Te}} = \frac{1 + \kappa_{T\mu} s}{1 + \kappa_{Te} s} = 1.008 \, {}^{+\,0.071}_{-\,0.063}$$

As one can see, all variables are consistent with the QED expectations within the quoted errors.

At the highest energies of PETRA ($W \geq 25$ GeV) one eventually has to apply a more sophisticated analysis of the data, since possible deviations from pure QED can also be caused by weak interaction effects. Work along these lines is underway. The results could also be affected by the existence of a longitudinal beam polarization (the effect of a transverse polarization would be cancelled by integration over azimuthal angle). Writing down the cross section for Bhabha scattering as

$$\frac{d\sigma}{d\cos\theta} = \frac{\pi\alpha^2}{2s} \left\{ \left(\frac{3 + \cos^2\theta}{1 - \cos\theta}\right)^2 + P_{\shortparallel}^{\,2} \left(\frac{1 + \cos\theta}{1 - \cos\theta}\right) (7 + \cos^2\theta) \right\} (1 + \delta_{rad}(s,\theta)) F^2_{S,T}$$

we have checked that even assuming a longitudinal polarization $P_{\shortparallel}$ as high as 50 % at all energies will influence the results on Λ in a negligible way (as shown in Table 3, line 4 for Λ_e).

In conclusion, we have measured Bhabha scattering in a wide energy range (from 9.4 to 31.6 GeV) and the reaction $e^+e^- \rightarrow \mu^+\mu^-$ at W = 9.4 GeV. The highest spacelike momentum transfer was -850 GeV^2. Due to charge identification we have been sensitive to the timelike cutoff parameter also in the reaction $e^+e^- \rightarrow e^+e^-$. We have found good agreement with QED predictions, when including terms up to α^3 and contributions from hadron and τ lepton vacuum polarization. In particular QED describes well the scattering angular distributions (Figs. 1,4), the acoplanarity distribution (Fig. 2), the absolute rates (Table 2) and the energy dependence (Figs. 1,3 and Table 3). We have put accurate and stringent limits on the validity of QED in terms of form factors and have tested the validity of some of the general principles which underly this and other field theories.

ACKNOWLEDGEMENTS

We gratefully acknowledge the outstanding efforts of the PETRA machine group. We are also indebted to the technicians of the service groups who have supported the experiment during data taking, namely our cryogenic group, the computer center, the gas supply group, the vacuum group and the Hallendienst. We like to thank our technicians for the construction and maintenance of the PLUTO detector. We acknowledge stimulating discussions with M. Greco. We are grateful to F.A. Berends and K. Sauerberg for providing us with their Monte Carlo program. The non-DESY members of the collaboration want to thank the DESY directorate for the support and hospitality extended to them.

REFERENCES

1. B. Bartoli et al.,
Nuovo Cimento 70A (1970) 615 and Phys. Lett. 36B (1971) 593
B. Borgia et al.,
Nuovo Cimento Lett. 3 (1972) 115 and Phys. Lett. 35B (1971) 340
V. Alles Borelli et al.,
Nuovo Cim. Lett. 2 (1971) 376 and Nuovo Cim. 7A (1972)330 and 345
M. Bernardini et al., Phys. Lett. 45B (1973) 510
F. Palmonari
Proceed. of the Int. Conf. on High Energy Physics,
Palermo (Italy), June 1975, pages 261-276

2. H. Newman et al.,
Phys. Rev. Letters 32 (1974) 483

3. DASP Collaboration, R. Brandelik et al.,
Z. Physik C1 (1979) 233
K. Sauerberg
Thesis, Internal Report DESY F22-79/01 (1979), unpublished

4. a) J.E. Augustin et al.,
Phys. Rev. Letters 34 (1975) 233
b) T. Himel et al.,
Phys. Rev. Letters 41 (1978) 449

5. L.H. O'Neill et al.,
Phys. Rev. Letters 37 (1976) 395
B.L. Beron et al.,
Phys. Rev. D17 (1978) 2187 and 2839

6. D. Barber et al.,
Phys. Rev. Letters 42 (1979) 1100
D. Barber et al.,
MIT Lab. for Nuclear Science Report 107 (1979), submitted to Nucl. Phys. B.

7. PLUTO Collaboration, Ch. Berger et al.,
Phys. Letters 81B (1979) 410

8. H. Jensing
Diploma Thesis, University of Hamburg (1977), unpublished

9. H. Daumann
Diploma Thesis
Internal Report DESY F14-78/05 (1978), unpublished

10. O. Achterberg et al.,
Nucl. Instruments 156 (1978) 287

11. H. Kapitza
Diploma Thesis
Internal Report DESY F14-79/01 (1979), unpublished

12. F.A. Berends et al.,
Nucl. Physics B63 (1973) 381
Nucl. Physics B68 (1974) 541

13. F.A. Berends, G.J. Komen
Phys. Letters 63B (1976) 432
In this paper the R value, which is the main parameter for computing hadronic vacuum polarization effects, was assumed to be ~ 5 at energies above charm threshold; since the present experimental value of R is ~ 4, the R value used in ref. 13 implicitly included the one unit contribution from τ pair production.

14. R.P. Feynman
Phys. Rev. 76 (1949) 769

15. R. Gatto
Proceedings of the Intern. Symposium on electron and photon interactions at high energies, Hamburg 1965, Vol. 1, p. 106
Deutsche Physikalische Gesellschaft, 1965

16. S.D. Drell
Ann. Phys. 4 (1958) 75

17. T.D. Lee, G. Wick
Phys. Rev. D2 (1970) 1033
N.M. Kroll
Nuovo Cim. XLV (1966) 65

18. K. Ringhofer, H. Salecker
Contribution to the 1975 Internat. Symposium on lepton and photon interactions at high energies, Stanford University
Stanford, California (unpublished)
and Contribution to the 19 th International Conference on high energy physics, Tokyo 1978, (unpublished)

19. PLUTO Collaboration, Ch. Berger et al.,
Z. Physik C1 (1979) 343

20. M. Gell-Mann and M.L. Goldberger
Phys. Rev. 96 (1954) 1433
L. Fonda and G.C. Ghirardi
Symmetry Principles in Quantum Physics,
M. Dekker, Inc. New York 1970

Table 1 Summary of corrections to the Bhabha cross-section

Identification efficiency	+ 0.7 ± 0.4 %
background	- 0.5 ± 0.2 % (E_{CM} < 20 GeV) - 0.9 ± 0.3 % (E_{CM} > 20 GeV)
possible event losses in data handling	$0 {+2 \atop -0}$ %
uncertainty of radiative correction	± 1.5 %
total systematic error in overall normalization*	± 4 %

* The cross sections for cos θ < 0.2 have an additional 6 % systematic uncertainty due to division of same sign pairs.

Table 2 Results of a fit to the Bhabha angular distribution. The first order QED angular distribution modified by radiative corrections and finite angular resolution was normalized to the data. The resulting values of χ^2/DF are given (DF = degrees of freedom). The table also lists the range of q^2 covered by the data and the ratio of the luminosities derived from the wide angle and small angle Bhabha scatters. The errors shown are statistical. The ratio has an additional systematic uncertainty of 9 %.

E_{cms} (GeV)	s (GeV^2)	q^2 range (GeV^2)	χ^2/DF (pure QED)	ratio of wide angle to small angle lumi.
3.0-4.8 (ref.4 a)	9 - 23	1.8 - 18.5		
9.4	88	8 - 75	19.4/24	0.987±0.022
13	169	16 -144	14.3/14	0.908±0.050
17	289	29 -246	9.03/14	1.042±0.051
22	484	48 -410	3.6/7	1.086±0.092
27.5	758	114 -644	9.6/15	0.894±0.034
30	900	135 -765	20.0/15	1.002±0.035
31.6	997	150 -847	12.9/11	0.935±0.055
average			89/100	0.964±0.018 ±0.09 (syst.)

Figure Captions

Figure 1 (a) - (f) The differential cross section $s\, d\sigma/d\cos\theta$ for Bhabha scattering at cms energies of 9.4, 17, 27.5, 30.6 and 31.6 GeV. The curves are the QED cross sections including the effects of radiation and finite angular resolution.

Figure 2 The acoplanarity distribution from Bhabha scatters at 9.4 GeV as compared to a Monte Carlo prediction (full curve).

Figure 3 The values of κ_e from a fit of eq. (1) to the Bhabha scattering data of Fig. 1 assuming $\kappa_S = \kappa_T$ (full points). The open point is from ref. 4a.

Figure 4 The differential cross section $s\, d\sigma/d\cos\theta$ for the reaction $e^+e^- \to \mu^+\mu^-$ at $E_{cms} = 9.4$ GeV (off resonance). The curve is the radiatively corrected QED cross section folded with the angular resolution.

Table 3 Fitted parameters and lower limits for the Λ parameters using different assumptions. Everywhere $\varepsilon = \pm 1$ represents the fitted sign in eq. (2) and $\Lambda_\pm$ corresponds to $\varepsilon = \pm 1$. The lower limit for Λ_+ (Λ_-) has been computed by χ^2 analysis from the corresponding positive (negative) upper limit for κ (e.g. $(\Lambda_+)_{\text{lower limit}} = (\kappa_{\text{upper limit}})^{-1/2}$). We have read off the 95 % c.l. values from the χ^2 curve, which can be asymmetric.

line	data used	E_{cms} (GeV)	assumptions	fitted parameters (GeV^{-2})	χ^2/DF	Lower limits (at 95% c.l.) for Λ's (GeV) $\Lambda_+ \geq$	$\Lambda_- \geq$
1	μμ	9.387	none	$\frac{\varepsilon}{(\Lambda_T^2)_\mu} = \kappa_\mu = .0003\ ^{+.0007}_{-.0006}$	6.4/10	21	30
2	ee	all energies (9.387, 13.0, 17.0, 22.007, 27.531, 31.572)	none	$\frac{\varepsilon}{(\Lambda_S^2)_e} = \kappa_{Se} = .000110\ ^{+.000064}_{-.000069}$	82/83	71	250
				$\frac{\varepsilon}{(\Lambda_T^2)_e} = \kappa_{Te} = .000003\ ^{+.000145}_{-.000150}$		71	78
3			analyticity and crossing symmetry ($\kappa_S = \kappa_T$)	$\frac{\varepsilon}{\Lambda_e^2} = \kappa_e = .000085\ ^{+.000054}_{-.000058}$	77/80	80	234
4			$\kappa_S = \kappa_T$ and $P_{\parallel}$ (beam polarization) = 0.5 at all energies	$\frac{\varepsilon}{\Lambda_{e,P}^2} = \kappa_{e,P} = .000084\ ^{+.000056}_{-.000060}$	82/84	79	230
5	ee and μμ	all energies	μe - universality ($\kappa_{Te} = \kappa_{T\mu}$)	$\frac{\varepsilon}{\Lambda_S^2} = \kappa_S = .000112\ ^{+.000064}_{-.000068}$	88/91	70	260
				$\frac{\varepsilon}{\Lambda_T^2} = \kappa_T = .000025 \pm .000168$		69	80
6			analyticity and crossing symmetry + μe-universality	$\frac{\varepsilon}{\Lambda^2} = \kappa = .000088\ ^{+.000058}_{-.000062}$	84/92	79	243

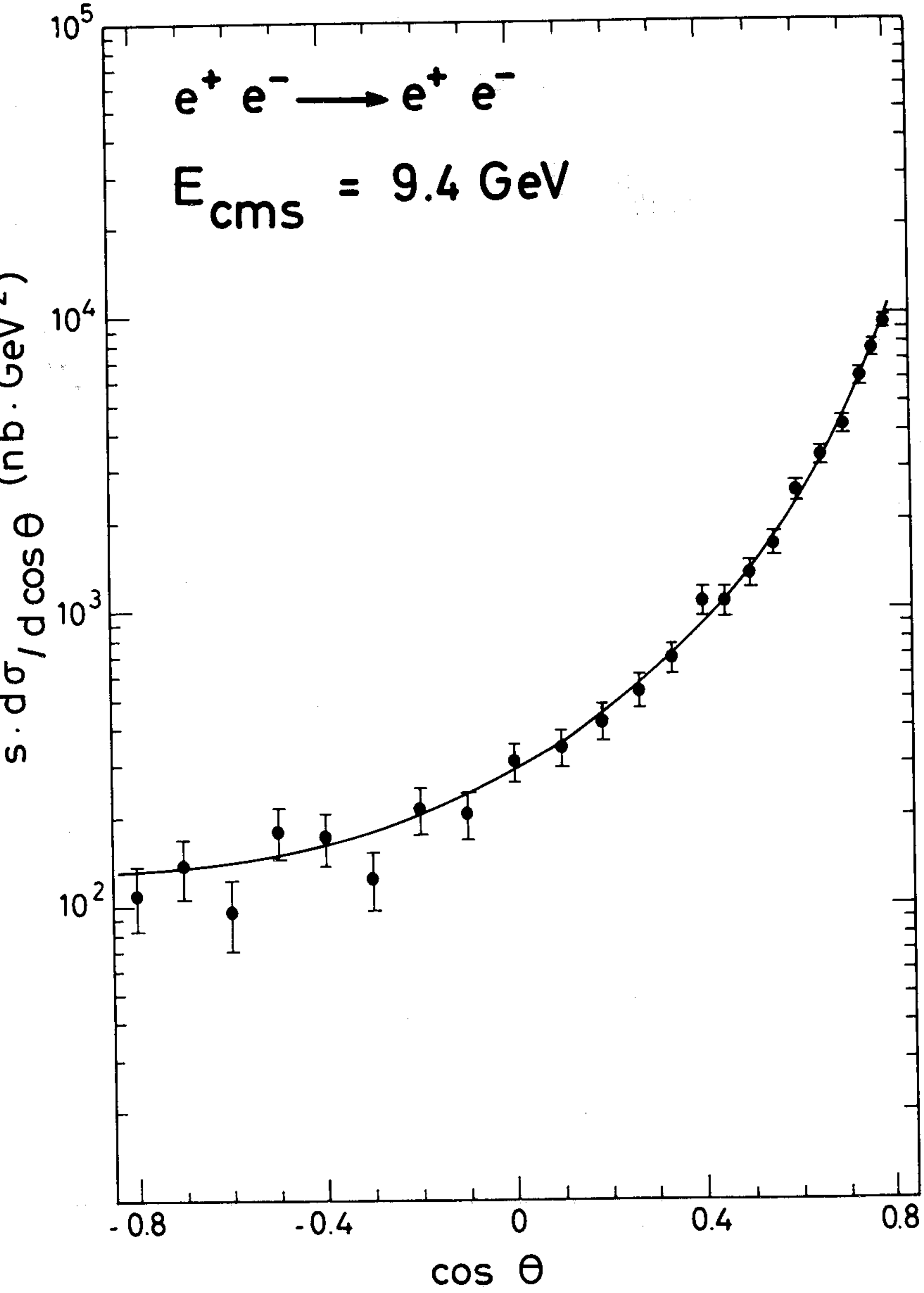

$e^+ e^- \longrightarrow e^+ e^-$
E_{cms} = 9.4 GeV
10^5
10^4
10^3
10^2
$s \cdot d\sigma / d\cos\Theta$ (nb · GeV^2)
- 0.8
-0.4
0
0.4
0.8
cos Θ

FIG 1 a

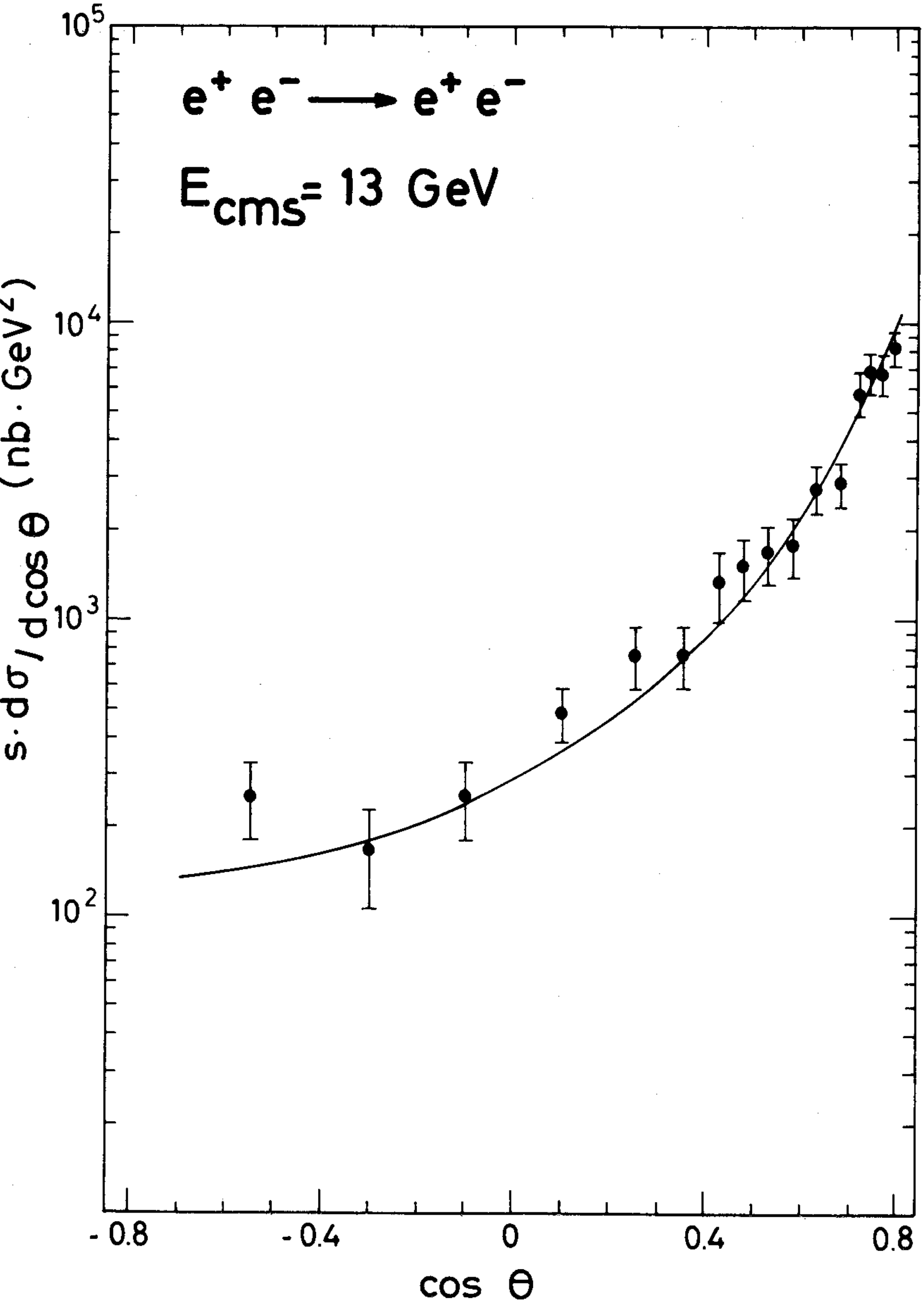

$e^+ e^- \longrightarrow e^+ e^-$
E_{cms}= 13 GeV
$s \cdot d\sigma / d\cos\Theta$ (nb · GeV^2)
10^5
10^4
10^3
10^2
- 0.8
-0.4
0
0.4
0.8
cos Θ

FIG 1 b

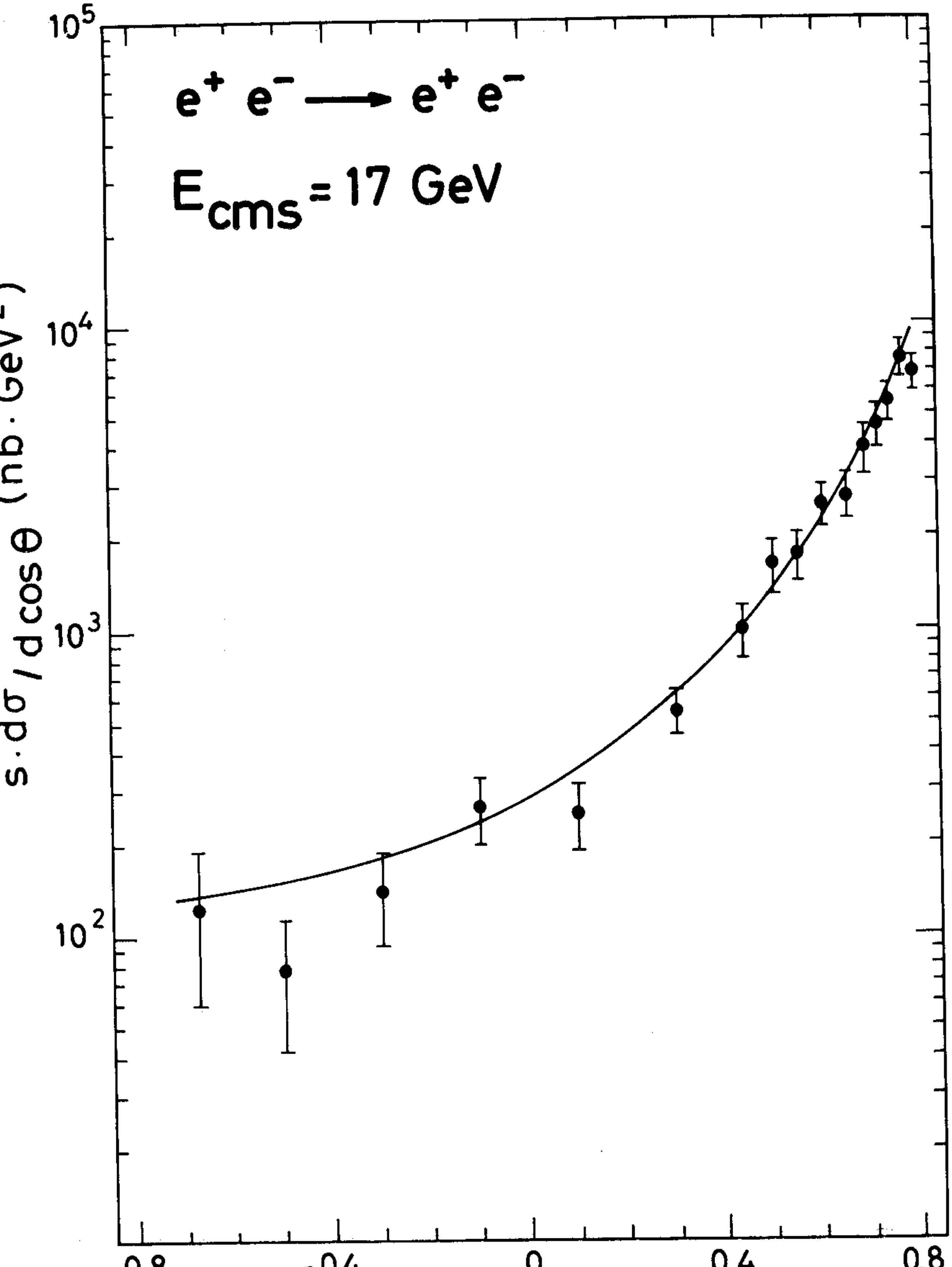

e+ e- ⟶ e+ e-
E cms = 17 GeV
s·dσ/dcosΘ (nb·GeV2)
10^5
10^4
10^3
10^2
- 0.8
-0.4
0
0.4
0.8
cos Θ

FIG 1 c

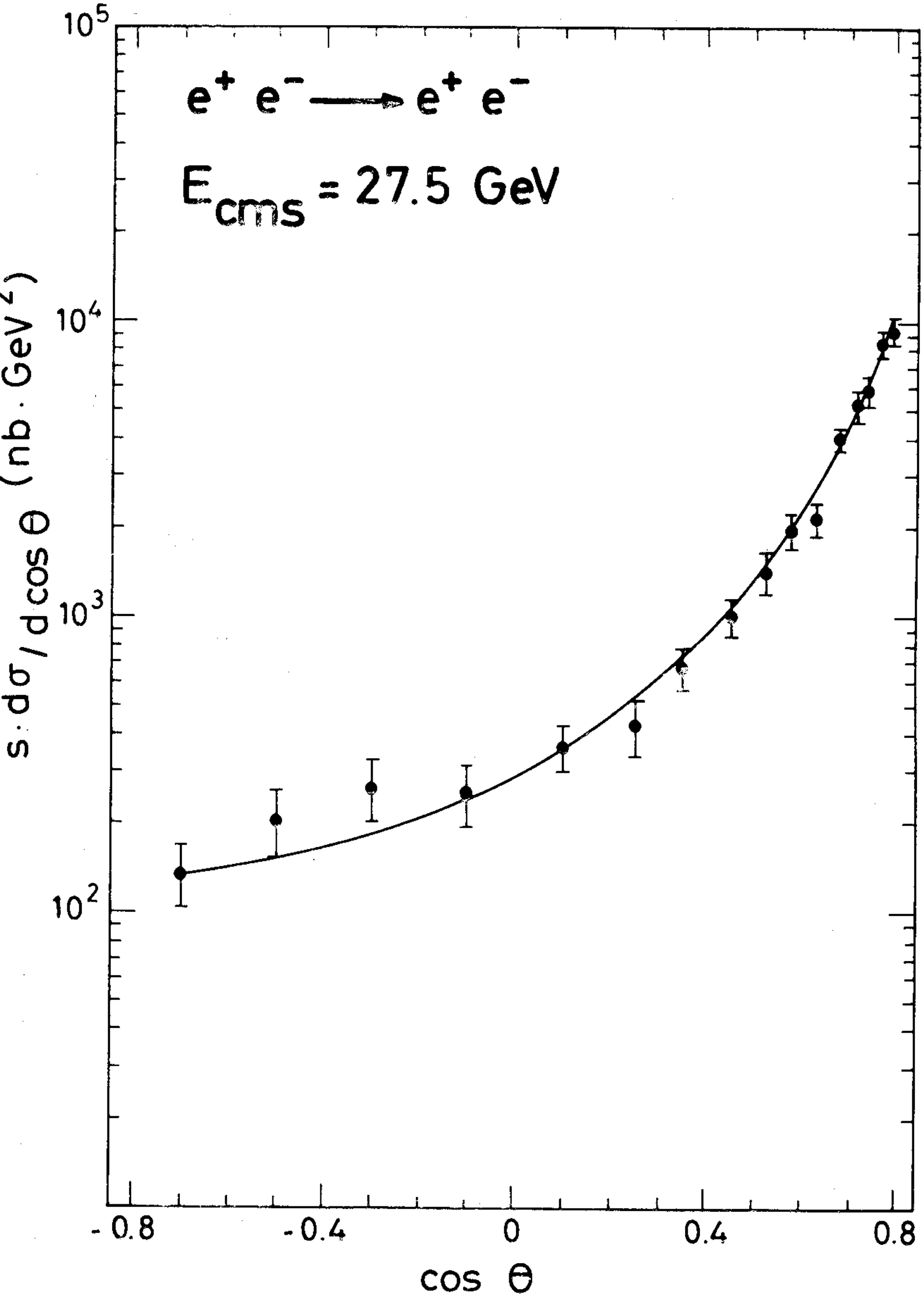

$e^+ e^- \longrightarrow e^+ e^-$
$E_{cms} = 27.5$ GeV
$s \cdot d\sigma / d\cos\Theta$ (nb · GeV^2)
10^5
10^4
10^3
10^2
- 0.8
-0.4
0
0.4
0.8
cos Θ

FIG 1 d

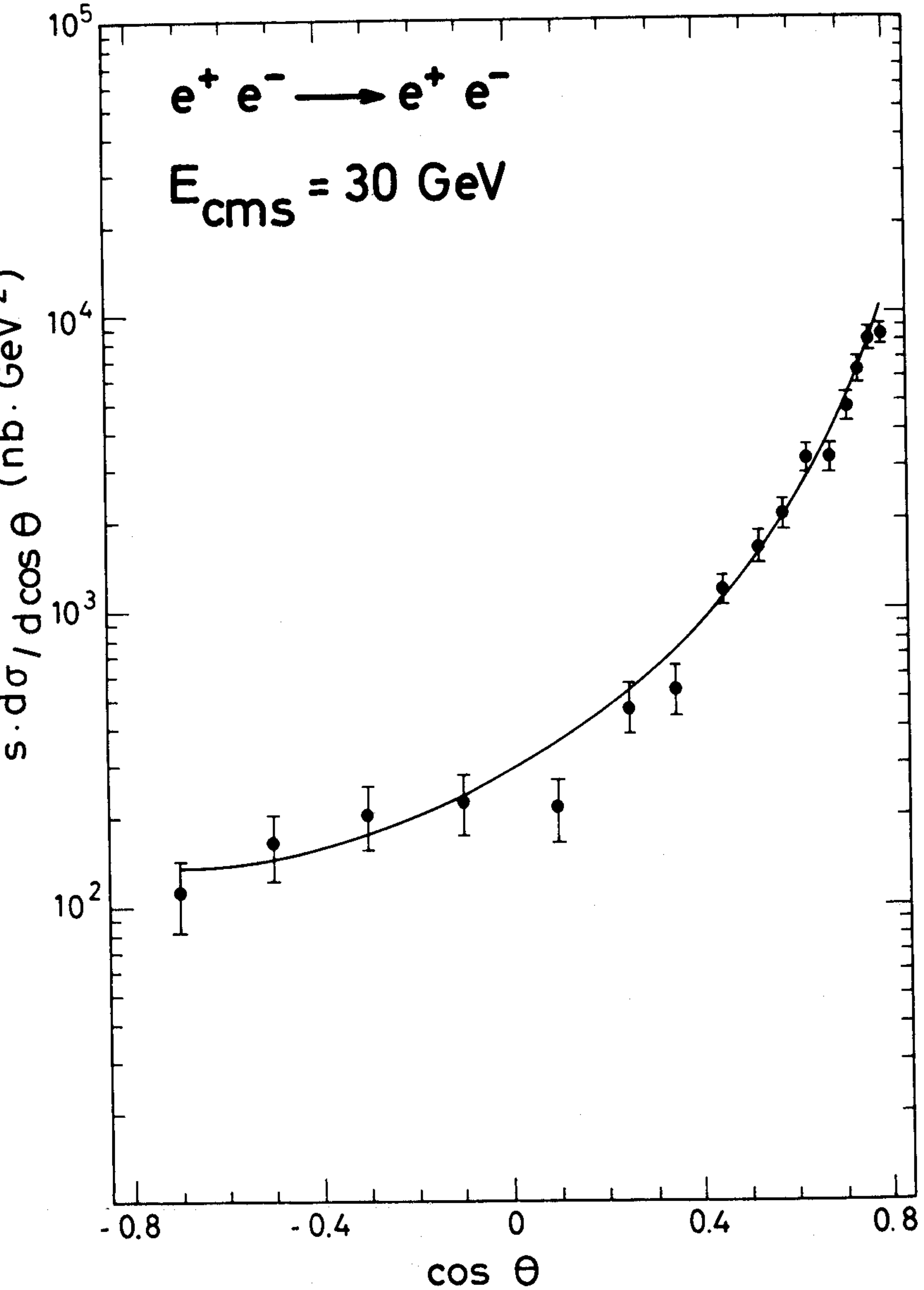
$e^+ e^- \longrightarrow e^+ e^-$
$E_{cms} = 30$ GeV
$s \cdot d\sigma / d\cos\Theta$ (nb · GeV^2)
10^5
10^4
10^3
10^2
-0.8
-0.4
0
0.4
0.8
cos Θ

FIG 1 e

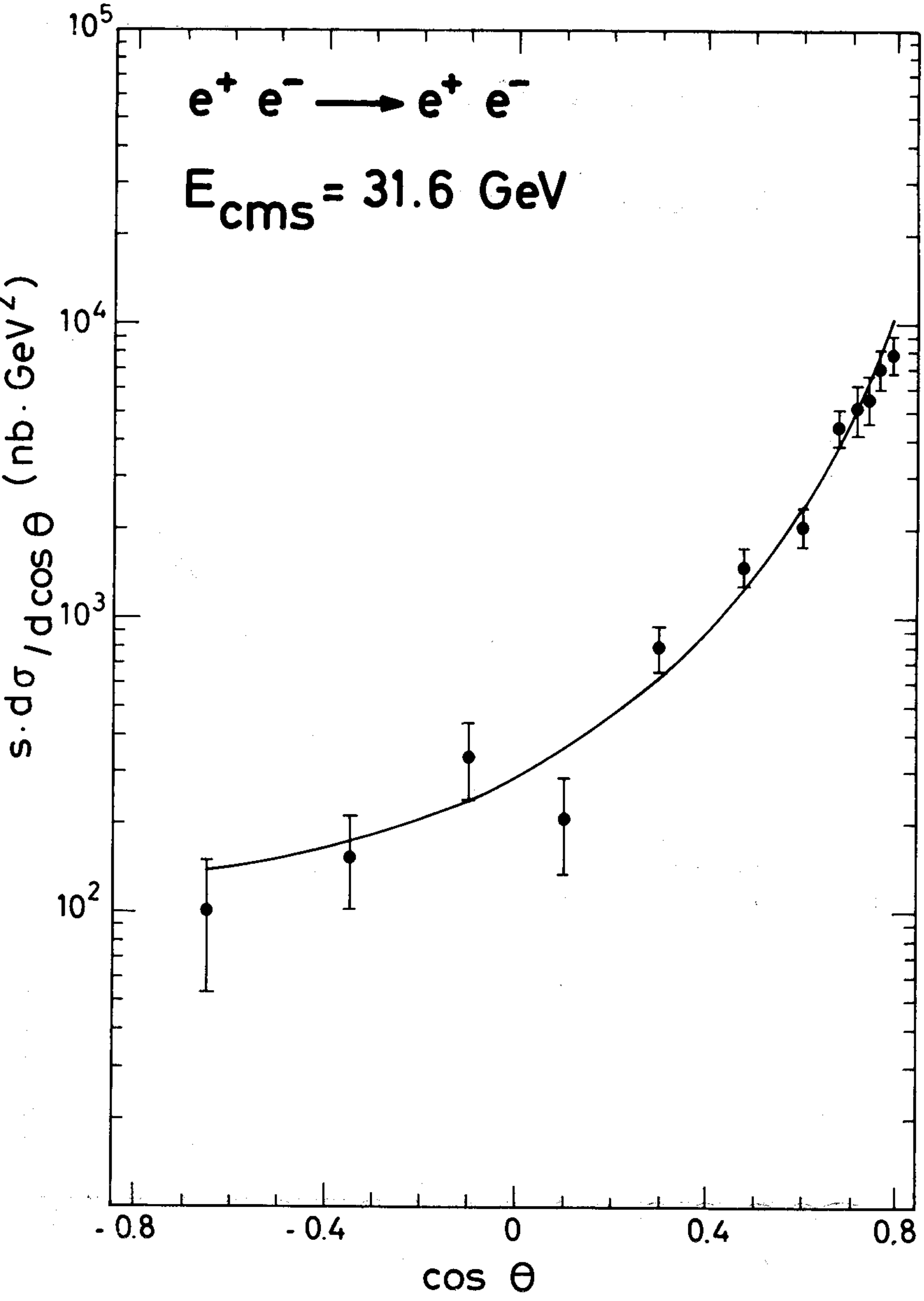

$e^+ e^- \longrightarrow e^+ e^-$
$E_{cms} = 31.6$ GeV
10^5
10^4
10^3
10^2
$s \cdot d\sigma / d\cos\Theta$ (nb · GeV^2)
- 0.8
- 0.4
0
0.4
0.8
cos Θ

FIG 1 f

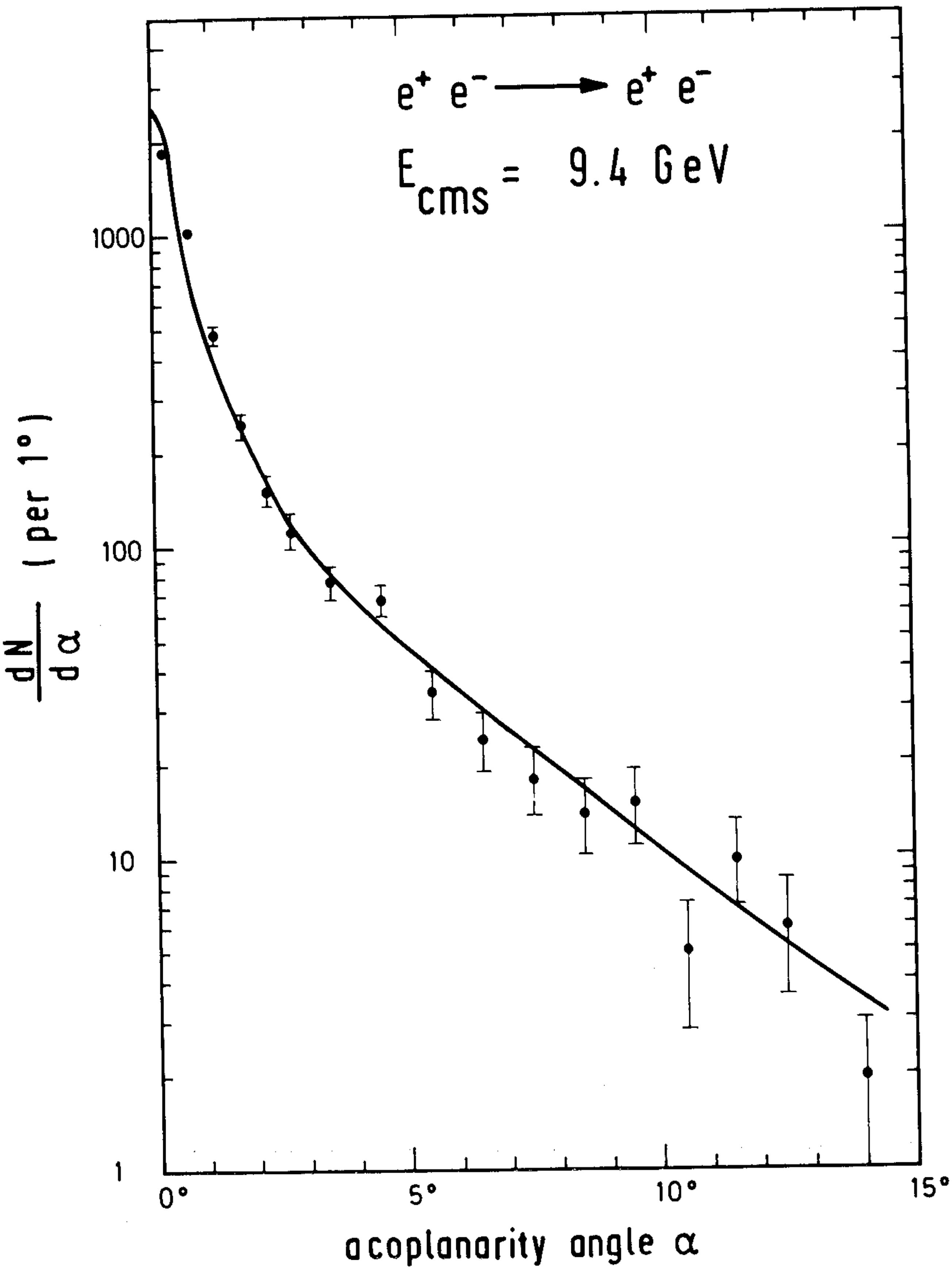

$e^+ e^- \longrightarrow e^+ e^-$
$E_{cms} = 9.4$ GeV
1000
100
10
1
$\frac{dN}{d\alpha}$ (per 1°)
0°
5°
10°
15°
acoplanarity angle α

FIG 2

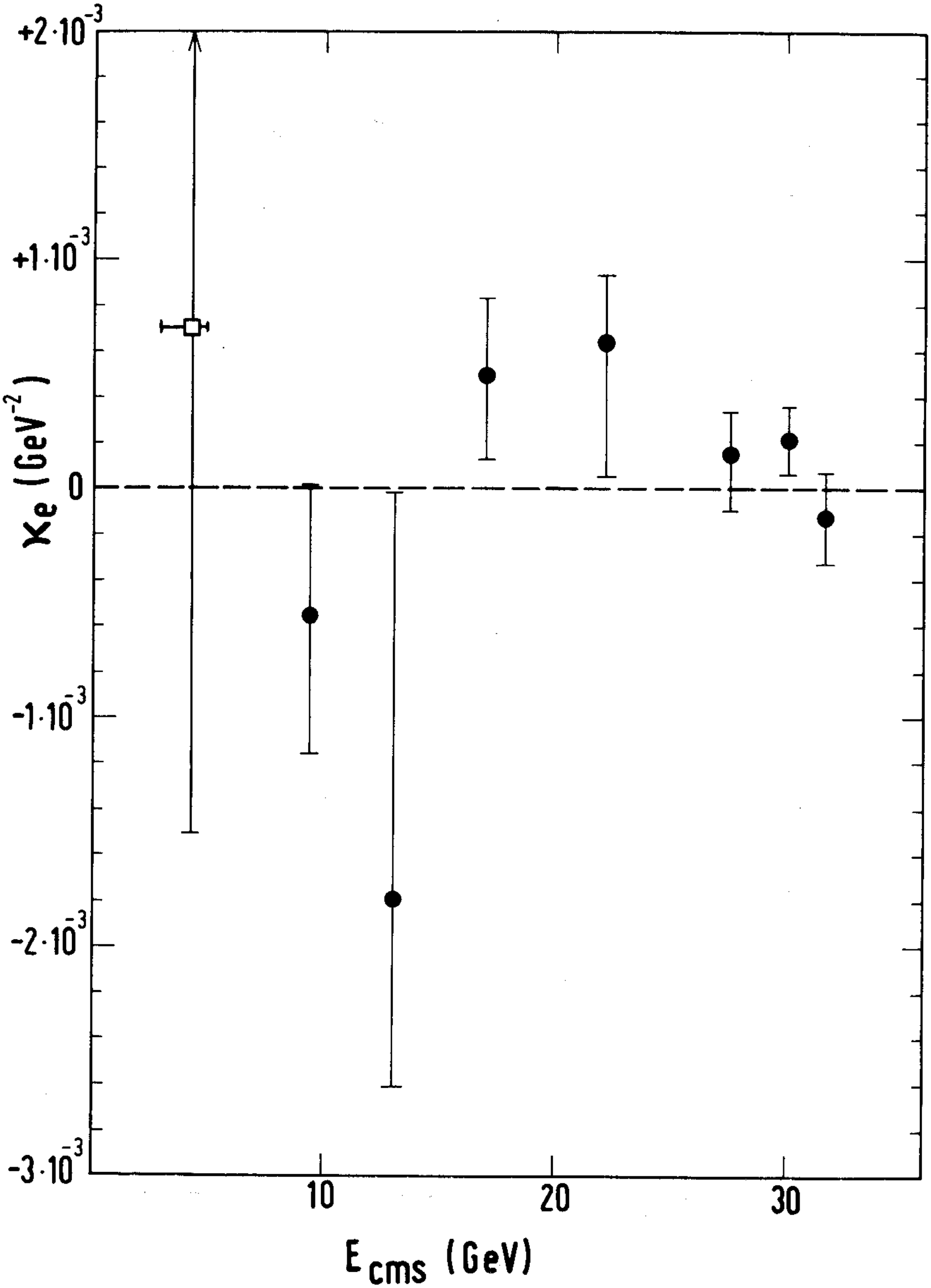

FIG 3

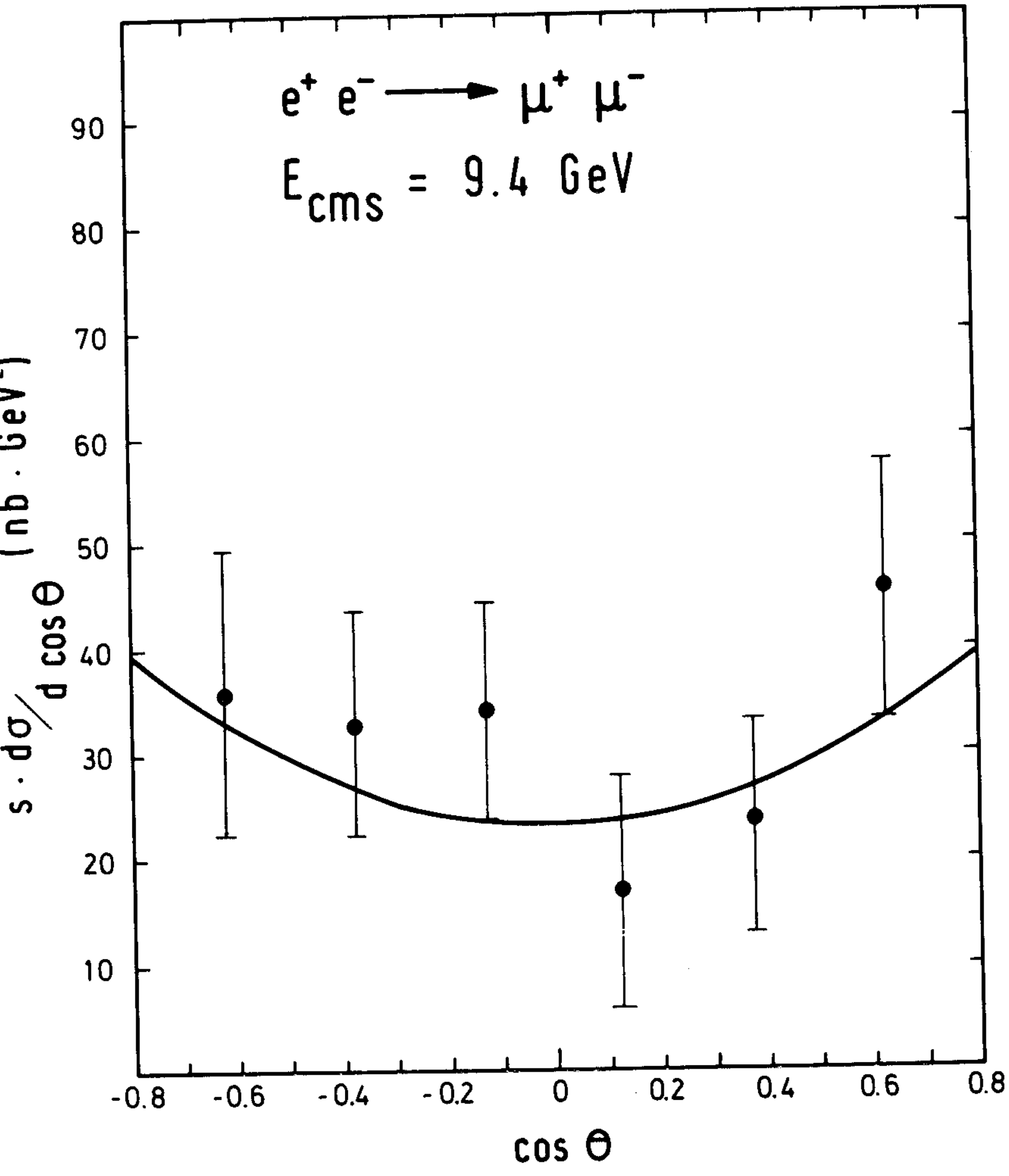

$e^+ e^- \longrightarrow \mu^+ \mu^-$
E_{cms} = 9.4 GeV
90
80
70
60
50
40
30
20
10
$s \cdot d\sigma/d\cos\Theta$ (nb · GeV^2)
-0.8
-0.6
-0.4
-0.2
0
0.2
0.4
0.6
0.8
cos Θ

FIG 4